Response-Time Measurements of Exciton and Pair Radiative Recombination Associated with the Zn-O Isoelectronic Complex in GaP, 4 to 100°K

J. S. Jayson and R. Z. Bachrach

Bell Telephone Laboratories, Murray Hill, New Jersey 07974

(Received 16 February 1971)

Experiments are described in this paper which increase our knowledge of radiative recombination in GaP(Zn, O) and which clarify several points of controversy that have recently arisen in the literature concerning the kinetics of GaP(Zn, O) luminescence. In particular, impulse-excitation experiments are described which yield an exciton-hole capture cross section of 10^{-14} cm^2 at 50 °K. Time-resolved spectral measurements verified this interpretation of the impulse experiments. This value is over three orders of magnitude greater than that deduced by previous workers. This result confirms that, at room temperature, exciton holes may reasonably be assumed to be in thermal equilibrium with valence-band holes, thus simplifying the description of excitonic recombination kinetics. Other experiments described here include a study of the nearly coincident exciton and pair red bands over the temperature range 4–100 ° K. These bands were separately observed using variable-intensity photoexcitation and spectral discrimination. The temperature-dependent time-decay behavior normally associated with the A and B transitions of an exciton bound to an isoelectronic center was observed for the first time in the GaP(Zn, O) system and the values $\tau_A = 35$ nsec and $\tau_B = 400$ nsec assigned. An upper bound on the pair-band strength was placed at $1.5 \times 10^{-13}(N_A - N_D)$ sec^{-1} on the basis of low-excitation-intensity time-decay measurements. Structure was observed on the usually featureless low-energy side of the red band in one crystal over a wide temperature range. A peculiar behavior observed in the time decay of the red band in the temperature range 60–80 °K is attributed to the thermalization of electrons from shallow donor levels at their subsequent recapture by the Zn-O complexes. This interpretation was substantiated by spectral and time-decay observations on the green pair band associated with the shallow donors. Finally, an explanation of the negative photoconductivity effect reported by Nelson and Rodgers at 20 °K is suggested, in which impurity conductivity, the dominant conductivity mechanism at this temperature, is decreased by the filling of ionized acceptor sites following photoexcitation.

I. INTRODUCTION

Isoelectronic impurities which act as radiative recombination centers for bound excitons have been identified in several semiconductors.[1-5] Oxygen on a Te site in ZnTe is an example.[2] In GaP such impurity centers include Bi and N and the nearest-neighbor complexes Cd-O and Zn-O.

Because of electron-hole j-j coupling, the zero-phonon line of the bound exciton is split ~1-3 meV and at low temperatures two lines are observed, the A and B transitions.[1] The B transition is nominally forbidden ($\Delta J = 2$) and its lifetime, along with that of its associated phonon replicas, is therefore much longer than that of the allowed ($\Delta J = 1$) A line. However, because the B line lies at a lower energy than the A transition, it can be observed at low temperatures (1.7 - 4 °K). As the temperature is raised, the A state is populated and the observed time decay is more rapid.

The behavior described above has previously been observed in several isoelectronic centers with the important exception of the Zn-O complex in GaP. Neither the zero-phonon lines nor the temperature-dependent time decay which should be associated with electron thermalization between the A and B transitions have been previously observed for this center. In Ref. 5, a lifetime of about 100 nsec was reported at both 1.7 and 20 °K, and the lack of temperature dependence attributed to mixing of the A and B states. We find that in low-concentration-doped samples, these transitions are not mixed. Thus, in the experiments reported here, the expected temperature dependence associated with the presence of A and B states has been observed in GaP(Zn, O).

A complication in the GaP(Zn, O) system is the presence of a pair band due to captured electrons on Zn-O complexes recombining with holes on Zn acceptor sites. This band is nearly coincident with the exciton band, but shifted ~25 meV to lower energies because of the difference in energies between the exciton-hole and acceptor-hole levels.[3-5]

In order to unambiguously separate radiation resulting from excitonic recombination from that due to pair recombination, it is necessary to either enhance the fraction of captured electrons on Zn-O sites which are associated with bound holes and thus study the exciton band, or suppress this fraction and study the pair band. We refer to the fraction of captured electrons associated with bound holes as the hole-occupancy factor and designate it $f(t, p)$, emphasizing that it depends on time and on excitation intensity, through the free-hole concentration

$p(t)$. If the exciton-hole capture and thermalization times are short compared with recombination times, this parameter is determined from steady-state and Fermi-statistics considerations.[5-8] However, at low temperatures the excited system does not satisfy these conditions, and the hole-occupancy factor can deviate substantially from the thermal-equilibrium value.

Since the available concentration of exciton-hole sites increases with excitation intensity while the concentration of the competing compensated acceptor sites decreases (because of saturation), a high excitation level favors the exciton band over the pair band.

The basic experimental technique utilized in this paper is the separation of the exciton and pair bands through intensity and energy discrimination. We study the exciton band using an intense focused exciting beam and observe emitted light on the high-energy side of the red band. Conversely, we study the pair band with a weak defocused beam and observe the emitted light on the low-energy side of the red band. In both situations spectral measurements are taken at all temperatures and the position of the peak of the red band is measured to ascertain whether the pair band or exciton band dominates.

Because of their pivotal importance in the kinetics of radiative recombination in GaP, we were particularly interested in obtaining the magnitude of the intrinsic exciton-radiation lifetime τ_{xr}, the relative strengths of the exciton and pair bands, and a reliable value for the capture cross section of the bound-exciton holes. With respect to obtaining this latter parameter, supplementary impulse-excitation and time-resolved spectral measurements were performed.

II. EXPERIMENTAL

A. Apparatus

The time decay and accompanying spectra were taken with a system[9] organized for photon-counting detection. The apparatus is capable of a 10-MHz counting rate and utilizes an RCA C31000E photomultiplier, a Didac 800 multichannel analyzer, and a Spex 1401 double monochromator. An argon-ion laser was pulsed with an acoustooptic modulator and the system was modulator limited to decay times greater than 2.5 nsec. The system timing accuracy was checked with mode-locked laser pulses and shown to be better than 0.5 nsec. Time decay was measured by the delayed-coincidence technique.[10]

In the delayed-coincidence technique, an ensemble of events consisting of the time differences between a trigger signal and the arrival of the first photon after the trigger signal is collected. The events are determined by a time-to-amplitude converter

and collected and displayed by the multichannel analyzer. In the limit that only one photon arrives per pulse and that there is an equal probability per channel of detecting a photon, the number of counts per channel is proportional to the intensity at the time corresponding to the channel.

Time-resolved spectra are obtained by placing a single-channel analyzer (SCA) after the time-to-amplitude converter. Only events within the time window defined by the SCA are collected in the spectra. The spectral resolution on all measurements was approximately 10 Å (5 meV).

Both the time-resolved and integrated spectra were taken with a pulsed beam so that the spectra taken corresponded to the spectra pertaining to the time-decay measurements. The samples were mounted in a Janis variable-temperature helium-gas-flow Dewar.

B. Crystal Data

Measurements were performed on a series of solution-grown (Zn, O) doped GaP p-type crystals. These crystals were doped in the melt with amounts of zinc ranging from 0.02- to 0.5-mole% Zn and with a fixed oxygen concentration of 0.02-mole% Ga_2O_3. Five crystals were investigated with net acceptor concentrations ranging from 4×10^{17} to 3.5×10^{18} cm^{-3}. In addition, three samples (from the same melt) which had received different thermal treatments were measured, one as-grown, a second annealed at 600 °C for 5 h, and a third raised to 1000 °C for 10 min and then quenched.

C. Heating Effects

For tightly-focused-beam experiments, sample heating can be a problem. Heating effects are difficult to isolate since lowering the intensity changes the relative strengths of the pair and exciton bands. Exciting pulse widths of 0.5 μsec were used for most of the measurements with a duty cycle of 0.006. The deflected laser power was about 300 mW. The focused spot size was of the order of 25 μm in diam. (Unfocused measurements refer to a spot size of several millimeters.) The low duty cycle was used to obtain accurate pair measurements as well as to minimize heating.

The temperature variation of the relative intensities of the A and B lines in well-understood isoelectronic systems, or the lifetime associated with these transitions, serves as a useful thermometer. The GaP(N) system was studied in Ref. 2 and using these results we performed lifetime measurements on a nitrogen-doped GaP sample under varying excitation conditions to study heating effects. While excitation with an unfocused beam resulted in no discernible heating, excitation with a highly focused beam led to transient temperature changes as high as 4 °K in the range 4°–10°K. These transient

temperature rises decayed within 150 nsec when 0.5-μsec excitation pulses were used and with proportionately shorter times, corresponding to smaller temperature rises, under narrower-pulse excitation.

Similar rapid transients were not observed in the focused-beam experiments on GaP(Zn, O) samples. Furthermore, by judicious variation of both pulse width and intensity and by comparison of the results from several samples, it was concluded that heating was not an important factor in these experiments.

III. EXPERIMENTAL RESULTS

A. Time-Decay Measurements
Emphasizing the Exciton Band

Samples were excited with the 4880-Å line of an argon-ion laser pulsed with an acoustooptic modulator. By focusing the beam and monitoring the high-energy side of the red band through the spectrometer we observed light predominantly from the exciton band. Spectral measurements verify this

FIG. 2. Time for the red luminescent intensity to decay to e^{-1} is plotted vs temperature for four samples with different doping levels. Samples are all strongly photoexcited and the emitted light at 1.91 eV is detected. Radiation due to excitonic recombination is thus emphasized. Solid curve represents the radiative time τ_{xr} as given by Eq. (1) and the parameter values in the text. At temperatures above $\sim 40\,°$K the decay mode changes from fast-excitonic decay to slow-excitonic decay, the latter characterized by the decay time τ_{xr}/f.
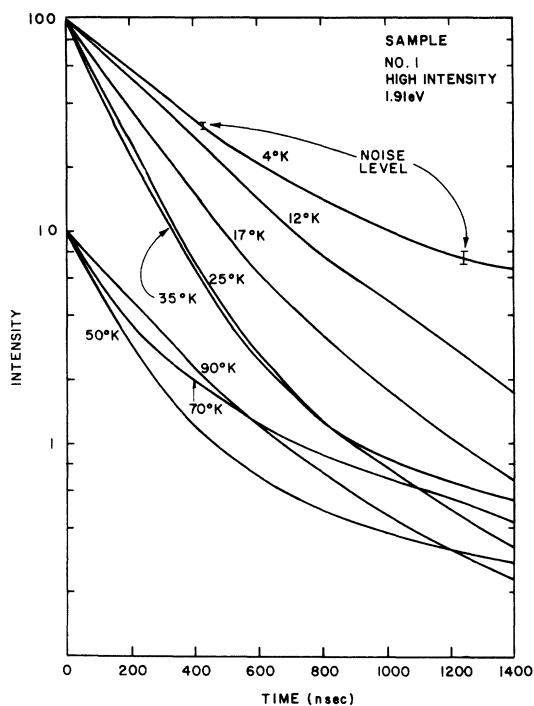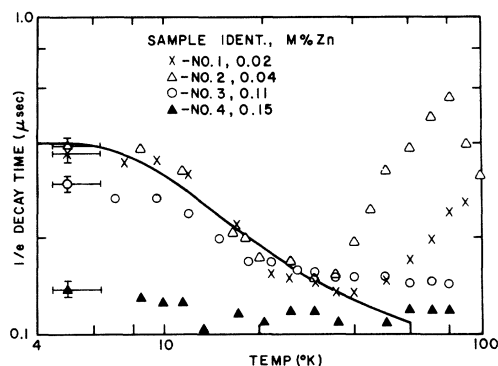
FIG. 1. Time-decay data with temperature as a parameter under conditions of high-intensity excitation. Emitted light is detected on the high-energy side of the red band (1.91 eV). Initial luminescence is exponential, representative of the exciton band, and gives a measure of τ_{xr}. In the temperature range 4–25 °K, the luminescence at later times represents the pair band while at higher temperatures the exciton band dominates throughout. Nonexponential character here is partially due to the influence of the pair band and partially to the change in character from τ_h to τ_D decay (see text).

conclusion. We estimate that a relative gain of between two and three is achieved for the exciton band over the pair band through inclusion of spectral discrimination in the time-decay measurements.

Typical results are given in Fig. 1, where logarithmic intensity is plotted as a function of time for several temperatures. The decay is exponential over nearly a decade in intensity. The nonexponential component is attributed in part to the pair band, and in part to the fact that there exist both a slow and a fast mode of excitonic decay. The fast mode may be understood as follows: When the excitation is sufficiently intense that conductivity modulation results, a large bound-exciton population is formed —with large fractional hole occupancy on electron-occupied traps. Following the termination of excitation, the free holes return to their equilibrium concentration leaving an excess bound-exciton population which then decays in the "fast" mode. The slow mode describes the decay of electrons captured by the Zn-O complexes under the condition that conductivity modulation is not important. The decay of these electrons is slow because the fraction associated with holes, to form excitons, is typically small. A more detailed discussion is given in Sec. IV. In Fig. 2, the $1/e$ decay times are plotted for several samples as a function of temperature. These samples range in net acceptor concentration from 4×10^{17} to 2×10^{18} cm^{-3}. The three least-doped samples exhibit similar behavior in the temperature range 4–30 °K, the time decay changing from about 300 to 400 nsec at 4 °K to about 150 nsec at 25 °K. Three samples from the same melt which had undergone different thermal treat-

ment also displayed the same temperature dependence. The time decay of the most highly doped sample depicted in Fig. 2 behaves similarly to crystals measured in Ref. 5 and exhibits little change in time decay over this temperature range. Another highly doped sample (0.5-mole% Zn) also showed this behavior. On these latter samples in addition to the initial decay of ~140 nsec, a longer exponential component of about 400 nsec was observed at the lowest temperature. A series of measurements with pulse widths ranging from 100 nsec to 1 μsec yielded the same results, indicating that heating effects were not a factor.

The temperature dependence illustrated in Fig. 2 in the 4–30 °K range is attributed to the increasing population of the A state with increasing temperature. The data can be fitted by the relationship[2]

$$\tau_{xr} = \tau_B (1 + g\,e^{-\Delta E/KT})/(1 + \gamma g\,e^{-\Delta E/kT}), \qquad (1)$$

where ΔE is the energy difference between the A and B states, $g = 0.6$, and $\gamma = \tau_B/\tau_A$. In the above it is assumed that the A and B states decay exponentially with time constants τ_A and τ_B, and have degeneracies of three and five, respectively. The parameter g is the ratio of these degeneracies. The theoretical curve in Fig. 2 was obtained using values of $\Delta E = 2.7$ meV, $\tau_A = 35$ nsec, and $\tau_B = 400$ nsec. [A value of $\tau_A = 100$ nsec was quoted in Ref. 5 from data on a crystal with mixed A and B states. The parameter actually measured, however, was τ_{xr} rather than τ_A. From our data and Eq. (1), we find a high-temperature limit of $\tau_{xr} = 85$ nsec and a room-temperature value of about 90 nsec, in good agreement with the data in Ref. 5.] An accuracy of ± 20% is assigned to the values of τ_A and τ_B. The value of ΔE is subject to larger error, since it is sensitive to temperature uncertainties. The corresponding values for the GaP(Cd, O) system have been obtained in Ref. 5 and are $\tau_A = 100$ nsec, $\tau_B = 600$ nsec, and $\Delta E = 2.1$ meV.

The time-decay temperature dependence observed on our more highly doped crystals, and in measurements reported in Ref. 5, is probably due to mixing of the A and B states as suggested by the earlier workers. Measurements of time decay vs temperature were also presented in Ref. 5 in which a low-temperature time-decay value of ~330 nsec was observed, but the characteristic decrease with rising temperature, as depicted in Fig. 2, was absent. This dependence indicates that the excitation intensity was not high enough to maintain the fast-excitonic-decay mode and the transition to the slow-excitonic-decay mode occurred before the population of the A state could be observed. The decrease in time decay for sample No. 2 at temperatures greater than 90 °K is attributed to an increase in the occupancy factor and the onset of

nonradiative Auger processes with increasing temperature.[5]

B. Time-Decay Measurements Emphasizing the Pair Band and Slow-Exciton Mode

Measurements taken with reduced excitation intensity favor the pair band at low temperatures. By defocusing the laser beam, the intensity was decreased by a factor estimated to be between 10^{-4} and 10^{-5}. Pair-band radiation was further preferentially detected by monitoring light on the low-energy side of the red band. As in the exciton measurements an excitation pulse width of 0.5 μsec was used and successive pulses were at 80-μsec intervals.

Logarithmic intensity as a function of time for the same sample illustrated in Fig. 1 is given in Fig. 3. As can be seen, the time decays are much longer with the lower excitation intensity. At the lowest temperatures, the long time decays are due to the dominance of the pair band, but at higher temperatures the exciton band dominates, and the long time decays are due to the exciton band decaying in the slow mode. In the range 4–25 °K, the time decay is temperature independent; the pair band dominates. With the onset of thermalization of holes into the valence band there is some mixing between the pair and exciton bands. This transition is marked initially by an increase in the $1/e$ lifetime, the 30 and 35 °K curves in Fig. 3, and then as the hole-occupancy factor f of the Zn-O complexes increases with increasing temperature, the measured lifetime decreases. Spectral measurements
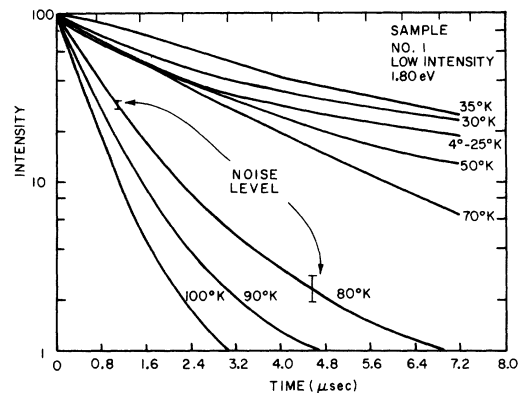
FIG. 3. Time–decay data with temperature as a parameter under conditions of low-intensity excitation. Emitted light is detected on the low-energy side of the red band (1.80 eV). Data are given for the same sample as in Fig. 1; note the different time scale. Single curve in the temperature range 4–25 °K represents the time decay of the pair band. At higher temperatures the exciton band dominates. This band decays with a time constant τ_{xr}/f (neglecting nonradiative processes) and the slow rate of decay at 30–35 °K reflects the low value of the hole-occupancy factor f at these temperatures.

indicate a shift from pair to exciton dominance coincident with the 25 °K transition temperature obtained from the time-decay measurements.

It is interesting that some other mechanism appears to affect the temperature dependence of time decay in Fig. 3 between 50 to 80 °K. Similar results were observed in the time-decay data of sample No. 2 given in Fig. 4. (Although there is no change in the time-decay curve between 4 to 50 °K in this figure, the peak of the integrated spectrum shifts from pair to exciton domination at 25 °K. Furthermore, time-resolved spectra taken at 45 °K indicate exciton-band dominance. In this latter experiment, emission was monitored in the interval 8–10 μsec after cessation of the excitation.) The abnormal increase in time decay between 50 and 70 °K can be understood by observing the spectrum of this sample taken under identical excitation conditions, as given in Fig. 5. We note that at 50 °K the green pair band[11] is the primary radiative band while at 80 °K this band is less intense than the red emission. From these data we conclude that electrons captured by shallow donor levels increasingly thermalize into the conduction band above 50 °K and that a fraction are recaptured by the Zn-O complexes. The logarithmic intensity of the green pair band as a function of time is plotted in Fig. 6. The tails of the red-band time-decay curves in this temperature range reproduce this time dependence (not apparent in Fig. 4 because of limited scale), confirming that electron thermalization out of shallow donor levels is responsible for the red-band time-decay temperature dependence in the range 50–80 °K.

An activation energy of ~90 meV was obtained from green pair time-decay data taken up to 100 °K. This value is reasonable when compared with the ionization energies of the probable (inadvertently
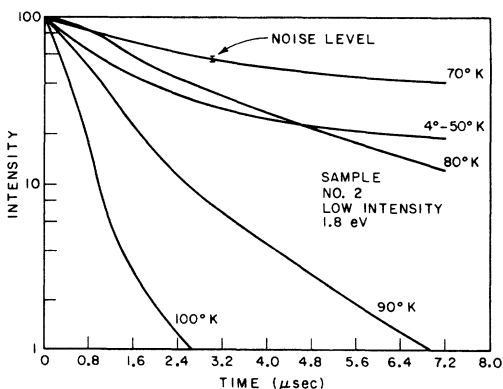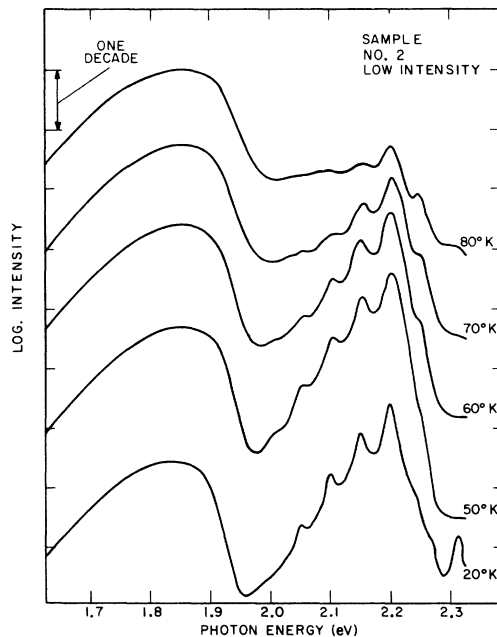

FIG. 5. Spectrum of sample No. 2 as a function of temperature. Curves have been displaced for clarity. Spectra are uncorrected for detector and grating response and the red band is approximately a factor of 2 higher than indicated relative to the green band. Excitation conditions are the same as in Fig. 4.

present) shallow donors; sulfur, 102 meV and silicon, 80 meV.[12]

From detailed balance, the thermalization time τ_{th} can be related to the ionization energy E_d and capture cross section σ_d through the expression
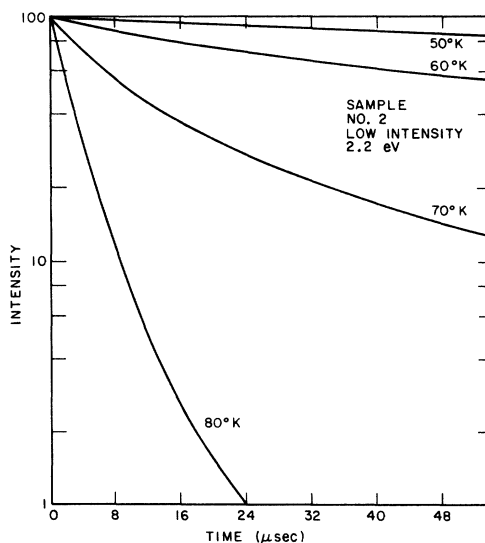

FIG. 4. Time–decay data with temperature as a parameter for sample No. 2. The conditions are the same as those in Fig. 3. The increase in lifetime between 50 and 70 °K is due to coupling with the green pair band.

FIG. 6. Time–decay data with temperature as a parameter for the green pair band of sample No. 2. Excitation conditions are the same as in Fig. 4.

$$\tau_{\mathrm{th}} = 2\, e^{E_d / kT} / N_c V_{\mathrm{th}} \sigma_d \,. \qquad (2)$$

At 100 °K, a range of values of $\sigma_d = 5 \times 10^{-14} - 5 \times 10^{-13}$ cm^2 is obtained for values of $E_d = 80-102$ meV. These large values explain the dominance of the green pair band at low temperatures despite the weak oscillator strength associated with the band.

We note that a slight energy dependence was observed for the green pair lifetime, the lifetime increasing with decreasing emission energy. We also observe that the nonexponential decay exhibited in Fig. 6 may be an indication of retrapping of electrons thermalized from yet deeper levels.

Structure was observed in the red band of one crystal in the course of studying low-excitation data. To our knowledge this structure has not been previously reported. This spectrum is given in Fig. 7. The structure persisted from 4 to 70 °K and was much more pronounced at low intensities than under high-excitation conditions where it was barely perceptible. The three sideband peaks on the low-energy side of the red band are separated by approximately 50 meV, while the main peak first sideband separation is closer to 75 meV. The shift in spectral position of the main peak between 19 and 40 °K arises from the change from pair-band domination to exciton-band domination. The sideband positions *do not* change in this temperature range, and thus we are led to conclude that this structure is not associated with the exciton band. The sideband energy interval is close to that of an LO phonon. [13]

C. Impulse Excitation and Measurement of Exciton-Hole Capture Cross Section

An experimental technique was described in Ref. 7 which exploited a luminescent material's response to short-pulse or impulse excitation. Briefly, the luminescent rise time is determined by the processes limiting the buildup of the radiating population. Thus, the electron minority-carrier lifetime limits the rise time of both the exciton and pair bands when the above band-gap excitation is used. In addition, the rise time of the exciton band is also limited by the equilibrium time of the captured exciton holes. Because the holes are the majority carriers, this time is also dependent on exciton-depletion terms and is given by $\tau_h = (\tau_{xr}^{-1} + \tau_{xp}^{-1} + p V_{\mathrm{th}} \sigma_{px})^{-1}$, where τ_{xp} is the thermalization time of holes back into the valence band, σ_{px} is the exciton-hole capture cross section, and p is the free-hole concentration.

At low temperature and high excitation rates, $p \gg p_0$ and the last term in the above expression can dominate. However, at low excitation levels the first two terms dominate and, if the minority-carrier lifetime is short, the rise time gives a measure of the hole equilibrium time τ_h.

We have performed impulse measurements on

several samples. In Fig. 8, time-response curves are given for two kinds of excitation: one intense (focused) and the other weak (unfocused); a 20-nsec excitation pulse was used in both cases. The focused beam generates a high free-hole carrier concentration resulting in a short capture time and in a short rise time. The luminescence decays in the fast-exciton mode.

The unfocused beam, however, does not significantly perturb the free-hole concentration and the rise time is thus the hole equilibration time, equivalent to the decay time of the focused-beam example. With unfocused excitation, the luminescence decays in the slow-exciton mode as in Fig. 3. Time-resolved spectral measurements which monitor the light 20 μsec after cessation of excitation verified that the exciton band was the dominant band. This is the clearest demonstration we have seen of the significant differences between the fast- and slow-exciton decay modes and of the importance of carefully distinguishing between them.

In Figs. 9(a) and 9(b), a series of low-intensity response curves are shown for samples Nos. 1 and 2. The excitation pulse is also depicted. The measurements were performed with excitation pulse widths of 10 to 20 nsec and with highly defocused beams. We estimate the total population of injected holes to be less than 10^{13} cm^{-3}. From published Hall data, [14] this perturbation does not result in significant conductivity modulation for temperatures of ~ 35 °K and higher.

At 35 °K, the luminescent intensity rises significantly during the excitation interval. This prompt
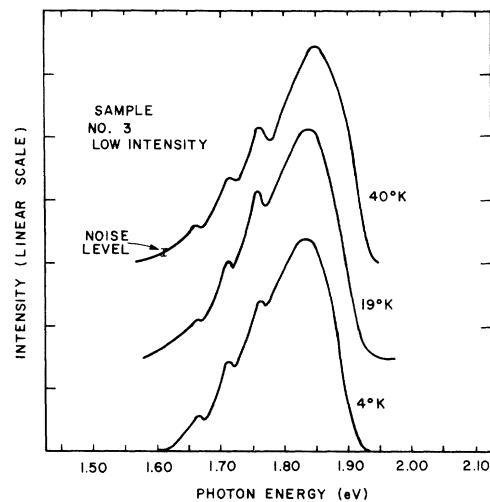

FIG. 7. Red photoemission spectra under conditions of low-intensity excitation. Spectra shown here are atypical with respect to the presence of structure on the low-energy side of the band. Structure persists to ~70 °K independent of whether the pair band or exciton band dominates.
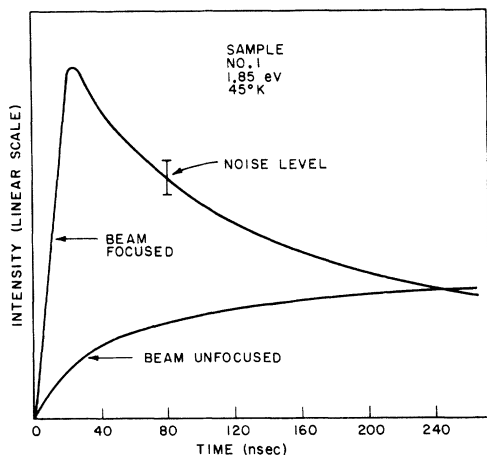
FIG. 8. Time-response data under conditions of impulse excitation with a 20-nsec laser pulse. Focused beam leads to a large perturbation from thermal-equilibrium conditions with the resulting fast rise time and fast-exciton mode decay. Much smaller perturbations generated by the unfocused beam yield the slow rise time (equal to the equilibration time τ_h) and a slow-exciton mode decay time (not depicted here).

radiation is indicative of a short minority-carrier lifetime and the presence of either a significant pair-band component or conductivity modulation. After excitation is terminated, a slowly rising component is observed which represents the equilibration time of the exciton band. This component increases in importance with increasing temperature and at 45 °K it is completely dominant. As the temperature is further increased, the rise time decreases until at ~ 55 °K it is equal to the excitation time. This latter decrease is attributed to the now-dominant exciton-hole thermalization term τ_{xp} which decreases in value exponentially with increasing temperature. The slightly different temperature behavior of samples 1 and 2 is attributed to differences in doping level with an accompanying small difference in ionization energy.[14] The interpretation of the results of Figs. 9(a) and 9(b) is buttressed by time-resolved spectral measurements performed at 55 °K. Measurements taken on light within 20 nsec of the initiation of excitation indicates that the luminescence is in the exciton band.

Measurements on the higher-doped sample No. 3 yielded excitation pulse-width-limited rise times over the temperature range 25–60 °K. There is evidence of tunneling from the acceptor sites to the exciton-hole site for higher-doped crystals[5] and the exciton-hole level also has a lower ionization level at the higher-doping levels,[14] from which it follows that thermalization is important at lower temperatures. Either of these two effects could account for the rise-time behavior of the higher-doped sample.
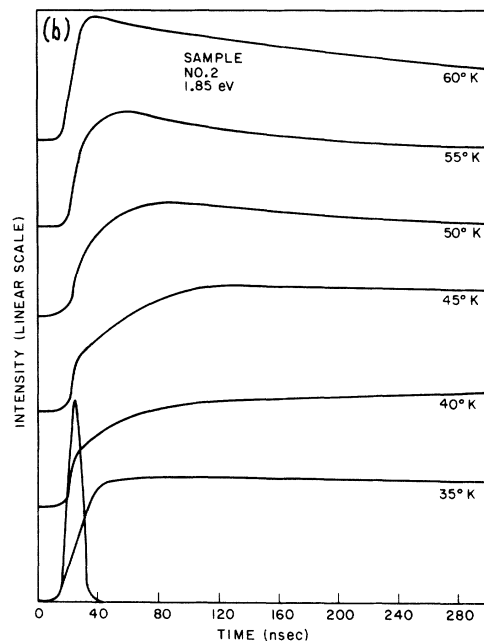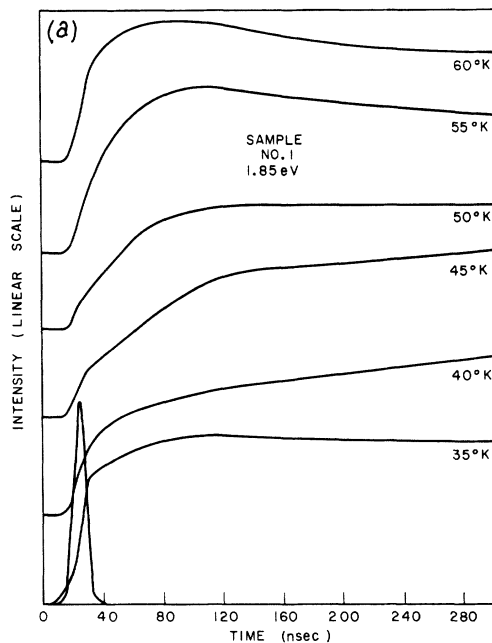

FIG. 9. (a) Impulse excitation under conditions of low excitation intensity for sample No. 1. Excitation pulse is also shown. Fast rise time at 35 °K represents either the pair-band or conductivity modulation. The slow rise time dominant at 40–50 °K is the equilibration time τ_h of the exciton band. Decrease in rise time at 55–60 °K is attributed to thermalization of holes from the bound-exciton level. A residual rise-time component other than the instrument time at 60 °K and higher temperatures may be an indication of the minority-carrier lifetime. (b) Same as (a). Measurements were performed on sample No. 2.

These rise-time measurements resulting from impulse excitation can be used to measure the exciton-hole capture cross section using the following procedure. As in Eq. (2), the exciton-hole thermalization time is related to the exciton-hole capture cross section through the expression

$$\tau_{xp} = 2\, e^{E_{ex}/kT}/N_v\, V_{th}\, \sigma_{px}\,, \tag{3}$$

where E_{ex} is the exciton-hole binding energy, N_v is the valence-band density-of-states function, and the factor of 2 is a spin-degeneracy factor. (The degeneracy due to heavy- and light-mass bands is split and can be neglected in the temperature range discussed here.) Using the data of the least-doped sample No. 1 at 50 °K, we find from Fig. 9 that $\tau_{xp} \sim 100$ nsec. Taking $E_{ex} = 35$ meV[3,4] and $N_v = 2.3 \times 10^{19}\,(T/300)^{3/2}$ we obtain a value of $\sigma_{px} \simeq 10^{-14}$ cm^2. This value is over three orders of magnitude greater than that deduced by Dishman and DiDomenico[8] from a multiparameter fit to the GaP(Zn, O) time-decay data in Ref. 5.

The reasons for the large discrepancy between our results and those of Ref. 8 include an improper solution of the initial-value problem obtained in Ref. 8. Also, it is difficult to obtain the exciton-hole capture cross section, given a proper theoretical solution, by fitting the temperature dependence of the time decay in GaP(Zn, O). This difficulty is illustrated in Fig. 10, where the time decay of sample No. 1 is plotted as a function of temperature for both high- and low-intensity excitation. The time-decay data of Ref. 5 fall between the high- and low-intensity extremes. As we shall see in Sec. IV, where the theoretical curves in Fig. 10 are discussed, the time decay in this temperature region is sensitive to the hole-capture cross section only when the exciton decays in the fast mode. Unfortunately, it has not been possible to maintain this decay mode to temperatures sufficiently high to observe exciton-hole thermalization.

The case of GaP(Cd, O), on which measurements were also reported in Ref. 5, is sufficiently different that the exciton-hole thermalization can be observed in the time decay. In contrast to the data on GaP(Zn, O), the dip in the time-decay–vs–temperature plot which GaP(Cd, O) displays is evidence not only of the B to A transition but also of hole thermalization. Because the A and B no-phonon transitions have been directly observed in emission in the (Cd, O) system,[5] the energy separation between the A and B states is accurately known. Thus we have been able to calculate the exciton-hole capture cross section for the Cd-O complex from these data and find a value of $\sim 10^{-14}$ cm^2 at 50 °K, similar to the value obtained for the Zn-O complex. These high values are reasonable for an attractive Coulomb center.[15]
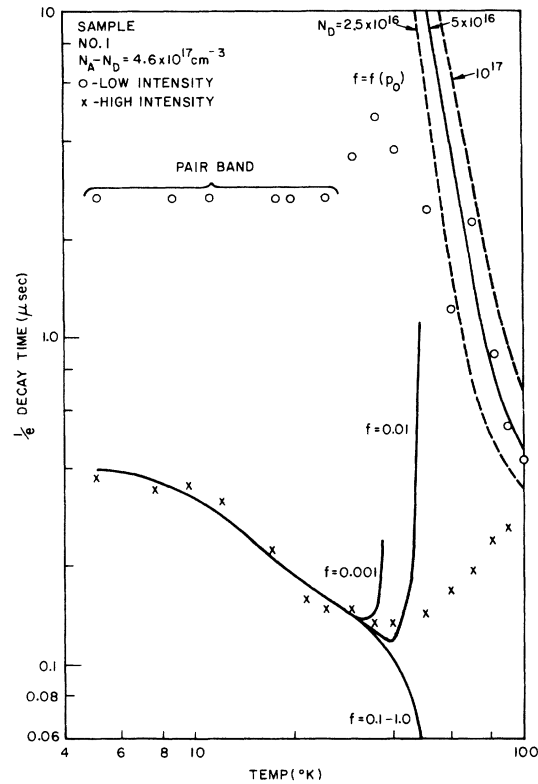

FIG. 10. e^{-1} time is plotted vs temperature for sample No. 1 under high- and low-excitation conditions. Curves were computed from Eq. (6b). The value of p_0 required in this calculation is obtained from the standard semiconductor expression

$$p_0 = \tfrac{1}{2}[\,-B + (B^2 + 4C)^{1/2}]\,,$$

where

$$B = N_D + N_v\, e^{-E_A/kT}/D_A$$

and

$$C = (N_A - N_D)\, N_v\, e^{-E_A/kT}/D_A\,.$$

The value of $N_A - N_D$ was obtained from Schottky-barrier measurements and is 4.6×10^{17} cm^{-3}. Acceptor degeneracy D_A is equal to 4 and $E_A = 60$ meV. Solid curve for $f = f(p_0)$ represents an estimated value of $N_D = 5 \times 10^{16}$ cm^{-3}. The two dashed curves represent calculations with $N_D = 2.5 \times 10^{16}$ and 10^{17} cm^{-3}. The value of $N_D = 5 \times 10^{16}$ cm^{-3} was used in the calculations of the lower curves. In computing the theoretical curves, a T^{-2} temperature dependence was assumed for the exciton-hole capture cross section. Upper curves are insensitive to this assumption while the effect of another choice on the lower curves would be a slight perturbation in the transition temperature.

IV. DISCUSSION

A. Analytic Solutions of Recombination Equations

Excitation of p-type crystals at low temperatures results in large-scale deviations from thermal equilibrium, and a solution of the transient problem must consider at least six different particle popula-

tions as indicated in Fig. 11. These populations consist of the free-electron concentration n, the ionized-donor concentration N_D^+, the captured electrons on Zn-O complexes N_t^e, the bound-exciton concentration N_t^x, ionized-acceptor sites N_A^-, and the free-hole concentration p. The donor sites are depicted schematically by both deep and shallow levels representing, respectively, oxygen and unintentional shallow donors such as sulfur. The exciton-hole level is indicated by a dashed line signifying the existence of this level only when a trapped electron occupies a Zn-O site.

A complete solution of the problem is not necessary for the discussion given here. We consider temperatures below 60 °K and hence neglect the coupling between the green pair band and the red band through thermalization of the shallow donor levels; the ionized-donor concentration N_D^+ need not be considered further. The minority-carrier lifetime is short and terms involving the minority-carrier concentration can be dropped. Also, specification of the ionized-acceptor concentration N_A^-, along with the appropriate equation (either a rate equation or neutrality condition), is not required. The remaining three equations are given in the Appendix.

A solution which closely approximates the experimental results depends heavily upon a correct specification of the initial conditions, which in turn depends upon detailed knowledge of relative values of capture cross sections, the extent of compensation, and the excitation intensity. Relatively short pulse widths were used experimentally and hence the steady-state solution does not necessarily satisfactorily describe the initial conditions for the decay problem. Rather than attempt a complete solution, we concentrate on two important limiting cases. First, an initial-value problem is considered from which it is demonstrated that the relative strengths

of the exciton and pair bands depend upon the excitation intensity. Second, the transient problem is considered in the limiting case of a time-independent free-hole concentration.

The initial-value problem consists of verifying a basic assumption throughout this paper that high excitation levels favor the exciton band over the pair band at low temperatures. This point has been made in previous papers,[5,8] but a simple demonstration is useful. In this example we assume steady-state conditions, very low temperatures (no hole thermalization), and, initially, low intensities such that $N_A^- \gg (N_t^e - N_t^x)$ are attained. Under these circumstances Eq. (A2) in the Appendix yields

$$\frac{N_t^x(0)}{N_t^e(0)} = \frac{p(0)v_{th}\sigma_{px}}{p(0)v_{th}\sigma_{px}+1/\tau_{xr}} , \qquad (4)$$

and from Eq. (A3) we find $p(0) \approx G_a/(N_A^-\tau_{pA}v_{th})$. Hence,

$$f(p(0)) \equiv \frac{N_t^x(0)}{N_t^e(0)} = \frac{(G_a/N_A^-)(\sigma_{px}/\sigma_{pA})}{(G_a/N_A^-)(\sigma_{px}/\sigma_{pA})+1/\tau_{xr}} , \qquad (5)$$

where σ_{px} and σ_{pA} represent the hole capture cross sections of the charged Zn-O complex and acceptor sites, respectively, and G_a is the excitation generation rate. The time dependence has been dropped from the exciton-hole—occupancy factor f since we will only discuss its initial value.

Equation (5) demonstrates that the occupancy factor increases with increasing excitation intensity. Furthermore, although the assumption $N_A^- \gg (N_t^e - N_t^x)$ is invalid at high excitation levels, from qualitative arguments it is concluded that f increases monotonically with increasing intensity.

Having briefly considered the initial-value problem, we next turn to an example of a solution of the transient problem. A derivation is given in the Appendix, whereby under the condition of $p(t) \approx p_0$, i. e., negligible modulation of the thermal-equilibrium free-hole concentration, the following solution is valid over a broad range of parameter space:

$$N_t^e(t) = N_t^e(0)\,e^{-t/\tau_D} , \qquad (6a)$$

$$N_t^x(t) = N_t^x(0)\,e^{-t/\tau_h} + \frac{f(p_0)N_t^e(0)}{(1-\tau_h/\tau_D)}\,(e^{-t/\tau_D}-e^{-t/\tau_h}) , \qquad (6b)$$

where

$$1/\tau_D = [1-f(p_0)]\textstyle\sum_r W(r)+f(p_0)/\tau_{xr}$$

and   (6c)

$$1/\tau_h = 1/\tau_{xr}+1/\tau_{xp}+1/\tau_{px} .$$

In these equations, τ_{xp} and τ_{px} represent the thermalization and capture times, respectively, of the exciton hole, and $\sum_r W(r)$ the pair-band strength. The summation over r refers to the position of all acceptor sites with respect to a Zn-O complex. If
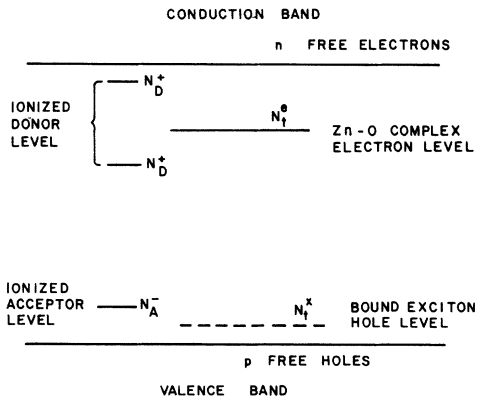

FIG. 11. Schematic representation of variable particle concentrations for the generalized low-temperature problem.

the initial conditions are such that $N_t^x(0) = f(p_0)$ $\times N_t^e(0)$ (implying that $p \approx p_0$ during excitation as well as the interval following excitation), then from Eq. (6b)

$$N_t^x(t) = \frac{f(p_0) N_t^e(0)}{(\tau_D - \tau_h)} (\tau_D e^{-t/\tau_D} - \tau_h e^{-t/\tau_h}) . \quad (7)$$

A response in the form of Eq. (7) is frequently encountered when linear networks are cascaded and an empirical decay time τ_D' of the form $\tau_D' = 1.05$ $\times (\tau_d^2 + \tau_h^2)^{1/2}$ provides a good measure of the observed decay time over a wide range of relative values of τ_D and τ_h.[16] Hence, when $N_t^x(0) = f(p_0) N_t^e(0)$ only the slow-exciton mode is observed.

The emitted light is related to the captured-electron and bound-exciton concentrations through the expressions

$$I_{ex} = \langle N_t^x(t)/\tau_{xr} \rangle , \quad (8a)$$

$$I_{pair} = \langle [N_t^e(t) - N_t^x(t)] \sum_r W(r) \rangle , \quad (8b)$$

$$I = I_{ex} + I_{pair} . \quad (8c)$$

The angular brackets in Eqs. (8a) and (8b) refer to an ensemble average of $\sum_r W(r)$ over all possible configurations to obtain the proper description of the the pair decay.[17] [The question of whether I_{pair} is proportional to N_t^e or $N_t^e - N_t^x$ is academic since $N_t^e \gg N_t^x$ and $1/\tau_{xr} \gg \sum_r W(r)$.]

B. Modes of Exciton and Pair Decay

Several observations are pertinent on the basis of Eqs. (6)–(8): (i) The exciton band exhibits two modes of decay, a fast mode with characteristic time τ_h and a slow mode with characteristic time τ_D. This result was previously deduced in Ref. 2. (ii) The pair band exhibits a single mode of decay τ_D. (iii) The exciton band dominates the pair band independent of excitation conditions when the condition $f(p_0)/\tau_{xr} > \sum_r W(r)$ is satisfied.

The fast-exciton mode represents an unloading of excess excitons formed during excitation, while the slow-exciton mode is an unloading of the excess captured electrons N_t^e through continued formation and loss of excitons while maintaining the relationship $N_t^x \approx f(p_0) N_t^e$.

From the discussion relating to Eq. (7) and examination of Eq. (6b), the fast-exciton mode is observed only when $N_t^x(0) \gg f(p_0) N_t^e(0)$, which implies $p \gg p_0$. Under these conditions Eq. (6) is only valid if the free-hole concentration rapidly returns to its equilibrium value upon termination of excitation.

The high excitation decay is thus qualitatively described by domination of the first term of Eq. (6b) $N_t^x(0) e^{-t/\tau_h}$ at very low temperatures and a transition to behavior described by Eq. (7) at higher temperatures. A detailed study of this transition region requires the solution of nonlinear equations.

In Fig. 10, limiting curves for high- and low-intensity excitation cases are given as calculated from Eq. (6b). The pair band is neglected in these calculations. The upper curves approximate the experimental condition for low excitation $[f = f(p_0)]$, while the lower contours were computed for constant initial-occupancy factors $[f = N_t^x(0)/N_t^e(0)]$. This latter condition is not experimentally satisfied since the generation rate is experimentally held constant as the temperature is varied. However, these contours, which are plotted over a range of f between 0.001 and 1.0, demonstrate that, as long as $f \gg f(p_0)$, the fast-exciton mode persists and the qualitative use of the expression "high excitation" throughout this paper is justified. As anticipated, the transition from the fast mode to the slow mode occurs when f approaches $f(p_0)$.

The upper curves were calculated using the standard semiconductor expression to obtain p_0. The net acceptor concentration $[N_A - N_D = 4.6 \times 10^{17}$ cm$^{-3}]$ was obtained from Schottky-barrier capacitance measurements. An exciton-hole degeneracy of $D_{ex} = 2 + 2 e^{-10/kT}$ was used as in Ref. 5 (units of kT are meV). Curves are plotted for different values of N_D and other than this quantity there are no adjustable parameters. The experimental points at 70 and 80 °K reflect the thermalization of shallow donors discussed earlier whereas the points between 30 and 50 °K can be explained by pair-band or conductivity-modulation influence. In general, the agreement between experiment and theory is satisfactory and the experimental points can be viewed as a measure of the occupancy factor.

We conclude this section with some comments on the difficulty of observing the thermalization time in the high-excitation-decay experiments as opposed to the impulse-excitation rise-time experiments. The onset of rapid thermalization of exciton holes occurs in the same temperature range as the transition from the fast-exciton to the slow-exciton decay mode, and the thermalization term which occurs in τ_h is subordinated by the τ_D term which does not explicitly depend upon the thermalization time. This difficulty does not manifest itself in the rise-time experiments. Another factor is the possible saturation of ionized-acceptor sites at high excitation levels, whence the thermalized holes may be recaptured by the Zn-O centers.

The puzzling observation by Nelson and Rodgers[18] of a negative photoconductivity effect in GaP(Zn, O) can tentatively be explained in terms of saturation of ionized-acceptor sites. The negative photoconductivity was observed after cessation of photoexcitation at 20 °K. Hall measurements in Zn-doped GaP[14] indicate that in this temperature range the primary conduction process is through impurity conductivity. The likely explanation of the negative photoconductivity effect is thus the saturation of

ionized acceptors and hence the removal of hopping sites.

C. Relevance for Room-Temperature Operation of GaP(Zn, O) Electroluminescent Diodes

This paper has thus far considered the low-temperature (4–100 °K) properties of radiation emitted by GaP(Zn, O). Some of the results, however, also have important implications for the description of room-temperature operation of red-emitting GaP electroluminescent diodes. To illustrate these implications it is instructive to recall several of the assumptions and estimates made in Ref. 5 regarding room-temperature radiation in the GaP(Zn, O) system: (i) The bound-exciton-hole population was assumed to be in thermal equilibrium with valence-band holes, equivalent to assuming that the thermalization time τ_{xp} is much shorter than other times of interest. (ii) The red pair-band strength was estimated to be $1.5 \times 10^{-13} (N_A - N_D)$ sec^{-1} (when all holes are on acceptor sites). (iii) A third red radiative band resulting from the recombination of electrons bound to Zn-O centers with free holes was assumed to have approximately the same oscillator strength as the pair (bound-hole) band, implying a transition rate of $\sim 1.5 \times 10^{-13} p$ sec^{-1}. Since the transition rate is proportional to the free-hole concentration, this band is expected to become important only at or above room temperature. It was then concluded that excitonic recombination is the dominant source of luminescence at room temperature (about an order of magnitude stronger than the combined pair and bound to free bands).

Subsequent work falls into two distinct categories, with one group of papers in substantial agreement with the above conclusions, [6,7,19,20] and with a second group[8,21–25] in basic disagreement with the crucial first point. The later work[24,25] in the second group is also in disagreement with the final conclusion that the exciton band is dominant—proposing instead that bound-to-free transitions are at least as important as excitonic transitions at room temperature.

The origin of these divergent approaches is found in the excessively small exciton-hole capture cross section deduced by Dishman and DiDomenico[8] from the time-decay data in Ref. 5. The acceptance of this low value in turn led to the conclusion that the hole thermalization time τ_{xp} is comparable to τ_{xr} and τ_{xn} and hence that the value of the fractional hole occupancy on the exciton

$$f(p_0) = 1/[1 + \tau_{px}(\tau_{xp}^{-1} + \tau_{xr}^{-1} + \tau_{xn}^{-1})]$$

at room temperature is substantially lower than the thermal-equilibrium value $f_0 = 1(1 + \tau_{px}/\tau_{xp})^{-1/2}$. (The parameter τ_{xn} is a nonradiative exciton decay time of importance at room temperature. See Refs. 6 and 7 for a detailed discussion of the room-

temperature problem.) When τ_{xp} is comparable in magnitude to τ_{xr} and τ_{xn}, separate equations are required to describe the kinetics of the electron and exciton populations on traps, N_t^e and N_t^x. [Both Eqs. (A1) and (A2) are thus required to describe the transient behavior.] Conversely, when the thermal-equilibrium value of f obtains, the exciton population is related to the total captured electron population simply by the expression $N_t^x = f_0 N_t^e$. One of the simultaneous equations describing the kinetics can therefore be eliminated and solutions much more expeditiously obtained and interpreted.

We have demonstrated in this paper that the exciton-hole capture cross section at 50 °K is $\sim 10^{-14}$ cm^2, over three orders of magnitude greater than Dishman and DiDomenico's value. Any reasonable extrapolation of this value to room temperature leads to the conclusion that $f(p_0)$ can to very good approximation be set equal to the thermal-equilibrium occupancy factor.

One concludes that the first assumption in Ref. 5 is valid and that the corollary of this assumption $N_t^x = f_0 N_t^e$ can be used[5–7,19,20] to simplify the theory of room-temperature recombination kinetics in GaP(Zn, O). It is then unnecessary to consider separately[8,21–25] the three charge states relevant for excitonic recombination at the isoelectronic impurity.

With regard to point (ii), an upper bound on the pair-band strength can be obtained from our low-excitation-intensity measurements. From Fig. 10, we observe that at 35 °K the decay time to e^{-1} of the initial intensity is ~ 5 μsec. If the pair and exciton band had equal transition rates in steady state at this temperature each of their strengths would be $\sim 10^5$ sec^{-1}. (By treating the pair band as if it decayed exponentially, its transition rate is overestimated in this discussion.) From spectral measurements, however, we know that the exciton band is actually stronger than the pair band at this temperature. Using this information together with the measured net acceptor concentration $(4.6 \times 10^{17}$ cm$^{-3})$ we arrive at an *upper bound* of $\sim 1.5 \times 10^{-13} \times (N_A - N_D)$ sec^{-1} for the pair-band strength. This bound is in agreement with the estimate from Ref. 5 and the conclusion that the exciton band dominates the pair band at room temperature is verified.

Finally, we discuss the bound-to-free band. The importance of this band was suggested by DiDomenico and Dishman[24] as a means of reinterpreting the impulse-response measurements of Jayson and Dixon.[7] These measurements, made at room temperature on GaP(Zn, O) electroluminescent diodes, showed fast luminescent rise times following impulse excitation. The radiation was assumed *a priori* to be excitonic and the rise times were then consistent with fast exciton-hole thermalization, but inconsistent with the small cross sections pre-

viously deduced by Dishman and DiDomenico.[8] Di-Domenico and Dishman then suggested[24] that bound-to-free radiation could account for the fast luminescent rise times and that their previous exciton-hole capture cross section results could still be correct. As has been unambiguously demonstrated in this paper, the latter is not the case. Thus no experimental evidence exists at present to support the suggestion that bound-to-free radiation is important at room temperature. We feel that in lieu of further evidence the qualitative arguments[5] leading to conclusion (iii) remain valid.

The discussion in this section is not academic. As demonstrated in Ref. 6, the exciton-hole–occupancy factor is a central parameter in the specification of room-temperature recombination kinetics and the optimization of quantum efficiency in GaP (Zn, O) material. The agreement between the upper theoretical curves and experimental points in Fig. 10, equivalent to a measure of the hole-occupancy factor, lends confidence to the room-temperature evaluation of $f(p_0)$ which cannot be directly observed. We are led to conclude that the best available estimates of the parameters pertinent for understanding the room-temperature quantum efficiency in GaP(Zn, O) are those contained in Ref. 6.

V. CONCLUSIONS

The motivation for this paper was to evaluate some of the fundamental parameters in the practically important red-emitting GaP(Zn, O) system. We have concentrated on characterizing this system below 100 °K, but some of the conclusions have important room-temperature implications as well.

By taking time-response measurements at high and low excitation intensities and by spectral discrimination, we have separately observed the nearly coincident exciton and pair red band in GaP (Zn, O). The exciton band was studied with the use of an intense focused excitation beam and the emitted light was detected on the high-energy side of the red band, which favors observation of excitonic recombination. The change of decay time from ~400 nsec at 4 °K to ~150 nsec at 25 °K was interpreted in terms of the equilibration of the A and B transitions associated with isoelectronic centers.

The pair band was studied with the use of a less intense defocused exciting beam and the emitted light was detected on the low-energy side of the red band, to favor observation of pair radiation. The upper bound of the pair-band strength was estimated to be $1.5 \times 10^{-13}(N_A - N_D)$ sec^{-1}. Previously unreported structure was observed on the low-energy side of the red band for one crystal using defocused excitation.

The exciton band was predominant at temperatures above 25 °K independent of excitation condi-

tions. A slow-decay mode characterized by the intrinsic exciton radiative lifetime divided by the fractional hole-occupancy factor τ_{xr}/f was observed with low-intensity excitation. This mode should be contrasted with the fast-decay mode, characterized by the intrinsic radiative time τ_{xr}, which was observed with intense excitation. Coupling between the green pair band and the red band was noted above 50 °K and a capture cross section in the range 5×10^{-14}–5×10^{-13} cm^2 obtained at 100 °K for the shallow donors associated with the green pair band.

Impulse-excitation measurements yielded an exciton-hole capture cross section of 10^{-14} cm^2 for the Zn-O complex at 50 °K. This value is over three orders of magnitude greater than the value deduced previously by Dishman and DiDomenico.[8] The interpretation of the impulse data was verified by time-resolved spectral measurements. From the time-decay measurements in Ref. 5, we have determined that the hole-exciton capture cross section for the Cd-O complex is also $\sim 10^{-14}$ cm^2 at 50 °K.

The magnitude of the exciton-hole capture cross section is used for the determination of the hole-occupancy factor f. Because the occupancy factor plays a central role in the recombination kinetics of the red band at room temperature, its evaluation has recently received much attention.[5–8] Any reasonable extrapolation of the capture cross section obtained here to room temperature leads to the conclusion that the room-temperature thermalization time is extremely fast and the approximation of setting the occupancy factor equal to the thermal-equilibrium value[5–7, 19, 20] is valid. This same conclusion was obtained from the room-temperature impulse experiments reported in Ref. 7.

APPENDIX

The recombination equations are given here for temperatures lower than ~60 °K, and nonradiative processes such as Auger processes are not included. The rate equations describing electrons trapped on the Zn-O complexes and bound excitons are[8]

$$\dot{N}_t^e = n\sigma_{nt} v_{th} N_t (1 - N_t^e/N_t) - N_t^x/\tau_{xr}$$

$$- (N_t^e - N_t^x)\sum_r W(r) , \quad \text{(A1)}$$

$$\dot{N}_t^x = (N_t^e - N_t^x)p v_{th}\sigma_{px} - N_t^x(1/\tau_{xp} + 1/\tau_{xr}) . \quad \text{(A2)}$$

In these equations, σ_{nt} and σ_{px} are, respectively,

the electron and hole capture cross sections of the Zn-O complex. The term $\sum_r W(r)$ represents the summation over all possible pair transitions for an electron captured in a Zn-O complex. The term $W(r)$ has the form $W_{max}\, e^{-2r/a}$, where a is the Bohr radius of a hole on an acceptor site.[17]

The expression describing the behavior of the free holes is

$$\dot{p} = G_a + N_t^x/\tau_{xp} - (N_t^e - N_t^x)p\sigma_{px}v_{th}$$

$$+ (N_A - N_A^-)/\tau_{Ap} - N_A^- p\sigma_{pA} v_{th} . \quad (A3)$$

Here, G_a is the generation rate, τ_{Ap} is the thermalization time constant from the acceptor level

$$\tau_{Ap} = 4\,e^{E_A/kT}/N_v\,\sigma_{pA}\,v_{th} ,$$

and σ_{pA} represents the capture cross section for holes by ionized-acceptor sites.

Consider an example in which the free-hole concentration p is assumed time independent. This condition is satisfied with increasingly higher excitation levels as the temperature is increased. We assume saturation of the Zn-O complexes is negligible. Upon cessation of excitation the free-electron population rapidly goes to zero and Eqs. (A1) and (A2) reduce to

$$\dot{N}_t^e + N_t^e\sum_r W(r) = - N_t^x[1/\tau_{xr} - \sum_r W(r)] \quad (A4)$$

and

$$\dot{N}_t^x + N_t^x/\tau_h = N_t^e/\tau_{px} , \quad (A5)$$

where

$$\tau_{px} = 1/(p_0\,\sigma_{px}\,v_{th}) , \quad 1/\tau_h = 1/\tau_{xr} + 1/\tau_{xp} + 1/\tau_{px} ,$$

and, from the steady-state solution of (A2), $f(p_0)$ $= \tau_h/\tau_{px}$. Combining Eqs. (A4) and (A5), we find

$$\ddot{N}_t^x + \dot{N}_t^x\,[1/\tau_h + \sum_r W(r)] + N_t^x\,[\sum_r W(r)/\tau_h$$

$$+ 1/\tau_{xr}\tau_{px} - \sum_r W(r)/\tau_{px}] = 0 . \quad (A6)$$

The solution to this linear differential equation is

$$N_t^x = A\,e^{S_1 t} + B\,e^{S_2 t} , \quad (A7)$$

$$S_{1,2} = -\tfrac{1}{2}\,[1/\tau_h + \sum_r W(r)] \pm \tfrac{1}{2}\,\{[1/\tau_h + \sum_r W(r)]^2$$

$$- 4\,[\sum_r W(r)/\tau_h + 1/\tau_{xr}\tau_{px} - \sum_r W(r)/\tau_{px}]\}^{1/2} .$$

The expression for $S_{1,2}$ can be expanded and we find

$$S_1 \simeq -\{[1 - f(p_0)]\sum_r W(r) + f(p_0)/\tau_{xr}\} = -1/\tau_D ,$$

$$S_2 \approx -1/\tau_h , \quad (A8)$$

and

$$N_t^x(t) = N_t^x(0)\,e^{-t/\tau_h} + \frac{f N_t^e(0)}{(1 - \tau_h/\tau_D)}\,(e^{-t/\tau_D} - e^{-t/\tau_h}),$$

$$N_t^e(t) = N_t^e(0)\,e^{-t/\tau_D} . \quad (A9)$$

These equations are discussed further in the text.

[1]D. G. Thomas, M. Gershenzon, and J. J. Hopfield, Phys. Rev. 131, 2397 (1963).

[2]J. D. Cuthbert and D. G. Thomas, Phys. Rev. 154, 763 (1967).

[3]T. N. Morgan, B. Welber, and R. N. Bhargava, Phys. Rev. 166, 751 (1968).

[4]C. H. Henry, P. J. Dean, and J. D. Cuthbert, Phys. Rev. 166, 754 (1968).

[5]J. D. Cuthbert, C. H. Henry, and P. J. Dean, Phys. Rev. 170, 739 (1968).

[6]J. S. Jayson, R. N. Bhargava, and R. W. Dixon, J. Appl. Phys. 41, 4972 (1970).

[7]J. S. Jayson and R. W. Dixon, J. Appl. Phys. 42, 774 (1971).

[8]J. M. Dishman and M. DiDomenico, Jr., Phys. Rev. B 1, 3381 (1970).

[9]R. Z. Bachrach (unpublished).

[10]W. R. Bennett, Jr., P. J. Kindleman, and G. N. Mercer, Appl. Opt., Suppl. 2, 35 (1965).

[11]M. Gershenzon, F. A. Trumbore, R. M. Mikalyak, and M. Kowalchick, J. Appl. Phys. 36, 1528 (1965).

[12]P. J. Dean, C. J. Frosch, and C. H. Henry, J. Appl. Phys. 39, 5631 (1968).

[13]P. J. Dean, Phys. Rev. 157, 655 (1967).

[14]H. C. Casey, Jr., F. Ermanis, and K. B. Wolfstirn, J. Appl. Phys. 40, 2945 (1969).

[15]M. Lax, Phys. Rev. 119, 1502 (1960).

[16]J. Millman and H. Taub, Pulse, Digital and Switching Waveforms (McGraw-Hill, New York, 1965), pp. 46-48.

[17]D. G. Thomas, J. J. Hopfield, and W. M. Augustyniak, Phys. Rev. 140, A202 (1965).

[18]D. F. Nelson and K. F. Rodgers, Phys. Rev. 140, A1667 (1965).

[19]W. Rosenzweig, W. H. Hackett, Jr., and J. S. Jayson, J. Appl. Phys. 40, 4477 (1969).

[20]A. Kasami, Japan. J. Appl. Phys. 9, 946 (1970).

[21]K. P. Sinha and M. DiDomenico, Jr., Phys. Rev. B 1, 2623 (1970).

[22]J. M. Dishman, M. DiDomenico, Jr., and R. Caruso, Phys. Rev. B 2, 1988 (1970).

[23]J. M. Dishman and M. DiDomenico, Jr., in Proceedings of the Tenth International Conference on the Physics of Semiconductors, edited by S. P. Keller, J. C. Hensel, and F. Stern (U. S. Atomic Energy Commission, Oak Ridge, 1970), p. 607.

[24]M. DiDomenico and J. M. Dishman (unpublished).

[25]J. M. Dishman, in International Election Devices Meeting, 1970 (unpublished).